9th International Conference on Hydrodynamics
October 11-15, 2010 Shanghai, China

Available online at www.sciencedirect.com
ScienceDirect
Journal of Hydrodynamics
2010, 22(5), supplement :330-336
DOI: 10.1016/S1001-6058(09)60214-6

www.sciencedirect.com/
science/journal/10016058

Development of an acoustic instrument for bubble size distribution measurement

Xiong-jun Wu [1*] , Georges L. Chahine[1]

[1]DYNAFLOW, INC. ,Jessup, Maryland, U.S.A
[*] E-mail: wxj@dynaflow-inc.com

ABSTRACT: Measurement of bubble size distribution and void fraction is of vital importance in many multi-phase flow applications. This paper describes an acoustics based device, the ABS Acoustic Bubble Spectrometer®, which can conduct measurements accurately in near real-time in a cost-effective fashion. By propagating short bursts of sound at different frequencies through bubbly medium, it measures frequency dependent attenuations and phase velocities of the acoustic waves and uses them to obtain the bubble size distribution (number of bubbles per size) by solving an inverse problem. Recent developments, both in hardware and software, as well as their validations are presented, these new advancements enable the ABS to measure void fractions up to $3x10^{-3}$ with bubble sizes ranging from 10 μm to 3mm.

KEY WORDS: bubble size distribution; void fraction; acoustic; multi-phase flow.

1 INTRODUCTION

Measurement of bubble size distribution and void fraction is very important in multi-phase flow applications that range from flows subject to cavitation occurrence and industrial processing, to oceanographic and biological flows. Several techniques have been used to-date to obtain such information [1-9], these techniques can be divided into optical methods (photography, holography, scattering, radiography, etc.), acoustical methods (scattering, attenuation, dispersion, etc.), and others (electrical impedance, cavitation susceptibility, etc). Acoustical methods are inverse methods, relying on the fact that bubbles have a strong effect on the propagation of acoustic waves. The acoustical cross-section of a bubble is three to four orders of magnitude greater than its geometrical cross-section [1]. Acoustical techniques are relatively simple, and applicable to much larger liquid samples and optically non-accessible media. Additionally, liquids are generally much more transparent to the passage of acoustic waves than they are to light.

Previous predictions of acoustical and optical techniques could differ widely [2]; for instance, the acoustical method of Wildt [3] over-predicts the bubble population density by as much as two orders of magnitude at small radii, and under-predicts it significantly at larger radii. The error lies in the procedures used to infer the bubble population from the measurements.

Using a set of effective equations, derived by taking the limit of the complete equations of motion to small bubble volume fractions [14], a dispersion relation for bubbly fluids was developed by Commander and Prosperetti [15]. This relationship was used to obtain the attenuation and phase velocity for given bubble populations and was compared very favorably with measurements. This study also found that the computed attenuations and phase velocities were quite sensitive to the bubble population distribution. Here, we use the inverse procedure and obtain two integral equations for the bubble population density in terms of the phase velocity and attenuation. Solution of these equations using measured values of the attenuation and change in phase velocity allows computation of the bubble population. The problem faced in the solution of these equations is that they are ill-posed, small errors in the measurement data have large effects on solution. We considered several approaches in previous studies for solving this ill-posed problem, and found that one based on constrained minimization and mathematical procedures to regularize the solution worked best [10-13].

2 BACKGROUND OF THE METHOD

2.1 Governing equations

The bubble size distribution in a bubbly medium is characterized by the bubble population density, $N(a)$, connected to M ,the total number of bubbles per unit volume with radii a between $[a_1, a_2]$ by:

$$\int_{a_1}^{a_2} N(a)\mathrm{d}a = M \tag{1}$$

When sound of frequency ω propagates through the bubbly medium, the bubbles oscillate, extract, and re-radiate energy into the medium. The effect of this dispersive behavior is to makes the sound speed in the mixture, C_m, complex. Each bubble acts as an oscillator with a characteristic natural frequency ω_0 and a damping constant b that depend upon the frequency of the imposed sound wave and the bubble radius. Damping due to viscosity, thermal effects, and acoustic re-radiation is considered in this case.

A dispersion relation that relates the complex sound speed in the mixture to the sound speed in the liquid, c_l, as a function of the bubble density , can be derived as follows, with i representing the imaginary unit:

$$\left(\frac{c_l}{C_M}\right)^2 = 1 + 4\pi c_l^2 \int_{a_1}^{a_2} \frac{aN(a)}{\omega_0^2 - \omega^2 + 2ib\omega}\mathrm{d}a. \tag{2}$$

This can be decomposed to obtain two new equations for $N(a)$ after separation of real and imaginary parts,

$$\frac{c_l}{C_M} = u - iv, \tag{3}$$

$$u^2 - v^2 - 1 = 4\pi c_l^2 \int_0^{\infty} \frac{\left(\omega_0^2 - \omega^2\right)a}{\left(\omega_0^2 - \omega^2\right)^2 + 4b^2\omega^2} N(a)\mathrm{d}a, \tag{4}$$

$$uv = 4\pi c_l^2 \int_0^{\infty} \frac{b\omega a N(a)}{\left(\omega_0^2 - \omega^2\right)^2 + 4b^2\omega^2}\mathrm{d}a \tag{5}$$

The quantities u and v can obtained by measuring the phase velocity, c_m , and the attenuation, A , of the acoustic wave in the bubbly medium. The phase velocity is related to u , and the attenuation, in dB per unit length, is related to v respectively by:

$$c_m = \frac{c_l}{u}, \qquad A = 20\lg_{10} e\left(\frac{\omega v}{c_l}\right) \tag{6}$$

Based on the above relationships, we regard u and v as sound speed ratio and attenuation respectively.

Notice that the two integral equations, Eq. 4~5, are Fredholm integral equations of the first kind with analytic, compact kernels, and are consequently ill-posed. Such an inverse problem is difficult to address as small variations in the measured quantities may results in large variations in the sought distribution.

2.2 Inverse problem solution

Among the techniques for achieving well-posed solutions to the inverse problem considered, the following method based on linear optimization was found to be most successful.

The integral equations, Eqs. 4-5, can be discretized and written in a standard linear system form:

$$\mathbf{KN} = \boldsymbol{\alpha}, \tag{7}$$

from which the bubble population density, **N**, can be solved using a simplex method by minimizing $|\mathbf{KN} - \boldsymbol{\alpha}|$ with appropriate constraints. In order to overcome the ill-posed character, the Tikhonov regularization method is utilized by replacing Eq. 7 with

$$\varepsilon\mathbf{N} + \mathbf{K}^T\mathbf{KN} = \mathbf{K}^T\boldsymbol{\alpha}. \tag{8}$$

$\mathbf{K}^T$ is the transpose matrix of $\mathbf{K}$, and ε is a small number compared to the maximum element of $\mathbf{K}$.

To validate the above numerical method, a set of sound speed ratios and attenuation data were obtained from Eqs. 4-5 with a prescribed density function $N(a)$, and were used as the input to the inverse problem solver. The prescribed $N(a)$ was a normal Gaussian distribution with 100 μm average radius and 10 μm standard deviation. The sound speed in the pure liquid was c_l =1500m/s. The minimum and maximum bubble radii were set to be 10 μm and 250 μm .

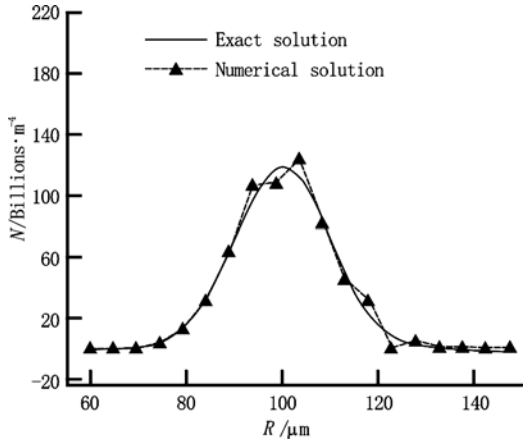

Fig. 1 Inverse solver solution without using regularization, c_l = 1500m/s

Fig. 1 shows the numerical solution when using the correct sound speed, 1500m/s, without using the

Tikhonov regularization and the solution compares well with the prescribed bubble population density function.

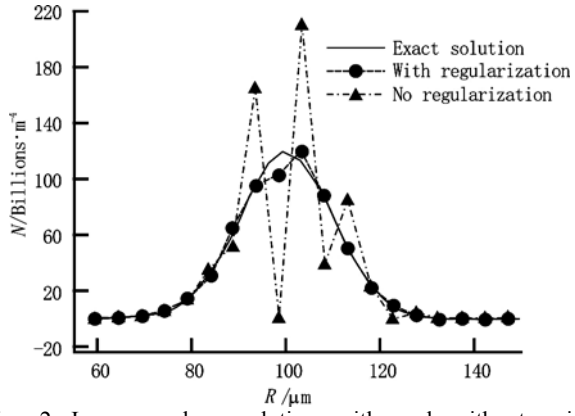

Fig. 2 Inverse solver solution with and without using regularization, c_l = 1468 m/s

Since the inverse problem is ill-posed, small errors in the input can lead to large errors in the solution. In the case of a small error in the liquid sound speed, e.g. c_l =1468m/s, Fig. 2 shows the numerical solutions from the inverse solver with and without using the Tikhonov regularization. The solution differs significantly from the prescribed bubble population density function without using regularization. However, with the regularization, the numerical solution is in good agreement with the exact solution.

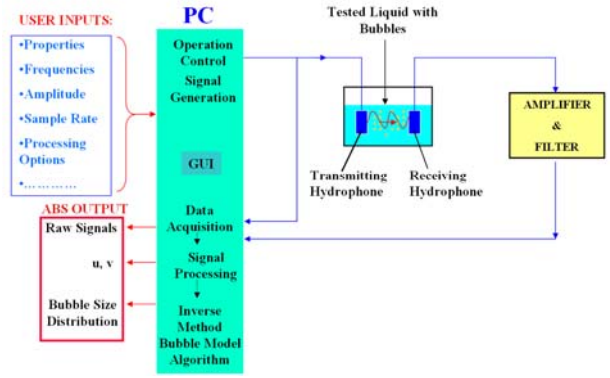

Fig. 3 Schematic of basic setup of ABS Acoustic Bubble Spectrometer®

2.3 The ABS acoustic bubble spectrometer®©

The ABS Acoustic Bubble Spectrometer®© extracts the bubble population from acoustic measurements of the phase velocity, c_m, and the attenuation, A, made at a range of insonifying frequencies. Fig. 3 shows a schematic of an basic ABS setup. It consists of a set of two hydrophones, one hydrophone is used for acoustic signal generation (emitter) and the other one is used for signal reception (receiver). A PC based high-speed data acquisition (DAQ) card is responsible for both generating the signals to drive the emitter and digitizing the received signals from the receiver. A signal amplifier is used to boost the received signals and an optional filter can also be used to filter out background noise. Utilizing specialized software algorithms, the received signals for a range of short single-frequency bursts of acoustic waves at different frequencies are compared with those from a reference liquid medium to obtain frequency dependent sound speed ratios and attenuations and, deduce the bubble size distribution by solving the inverse problem. All measurement operations, such as data acquisition, analysis, and results screen display are user controlled with a user friendly Graphical User Interface (GUI).

3 ACOUSTIC SIGNAL MEASUREMENTS

3.1 Frequency range expansion

Each hydrophone has its best signal response around its resonance frequency, the response decays as the frequency deviates from the resonance frequency. Fig. 4 shows the frequency response curves of three different sets of hydrophones, which clearly indicates that no single hydrophone can cover a broad frequency range. However, in some applications, the bubble size range can cover a broad range from a few microns to several millimeters or higher.

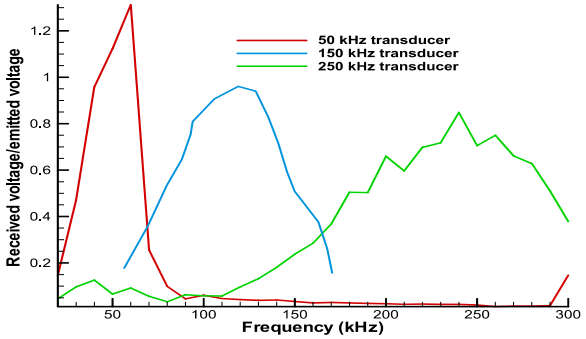

Fig. 4 Variation of signal response with frequency for three sets of hydrophones used in the ABS system with different resonance frequencies

One way to address this, as suggested in Fig. 4, is to use multiple sets of hydrophones with different resonance frequencies to cover the broader frequency range with good signal response. This has resulted in our development of an ABS system that supports multiple-set hydrophones. Fig. 5 shows a sketch of such a setup with three hydrophone pairs, e.g. with resonance frequencies at 50 kHz, 150 kHz, and 250 kHz. Due to the limited number of available analog output channels on a multi-functional DAQ card, a programmable multiplexer switch is used to route the emitted signal to the desired transmitting hydrophone pairs based on the emitted frequency. One set of hydrophones is active at a time and the acoustic interference among hydrophone sets is minimized.

Fig. 6 shows a picture of an ABS system with triple-set hydrophone support. The number of sets can be customized to meet specific application requirements.

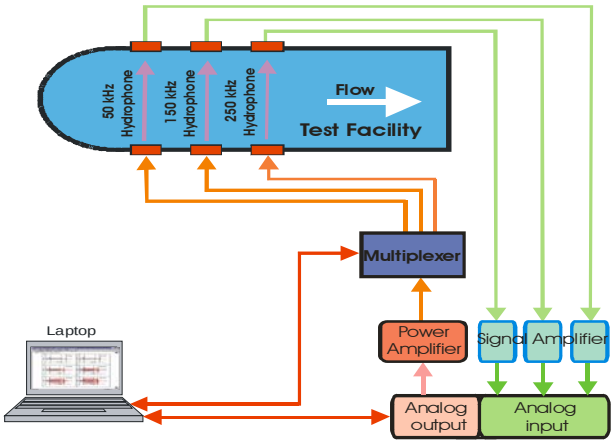

Fig. 5 Schematic of setup for an ABS system with multiple sets of hydrophones

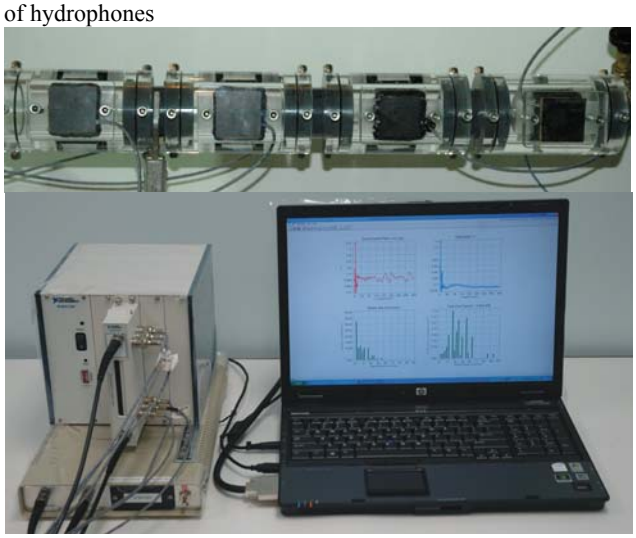

Fig. 6 Setup of a triple-set ABS system

3.2 Improvement of signal quality

3.2.1 Effects of amplified signal emission

The multi-functional DAQ card utilized in the ABS system can generate a maximum 20-volt peak-to-peak analog signal, which could be too low for good measurements in large void fractions. To address this issue, the ABS system can be coupled with an external broad bandwidth power amplifier to boost the analog output signal from the DAQ and send it to the transmitting hydrophone (Fig. 5). Since only signals in the bubbly medium needs to be amplified, the data analysis automatically takes into account the difference between the reference and test signals. Fig. 7 shows the effect of the amplification on the results, use of a power amplifier provides significant improvements on the measurement for the low frequencies and allows detection of larger bubbles.

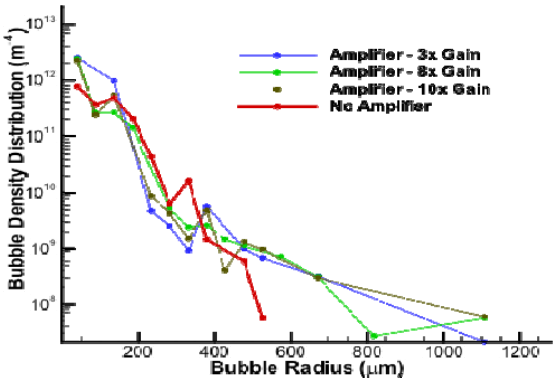

Fig. 7 Effects of the amplified emitted signal on the measurements

3.2.2 Signal generation and acquisition optimization

Since the amplitude response of a hydrophone varies significantly with frequency, the analog signal output from the DAQ card needs adjustment to avoid very weak signals or saturation. Also, the data acquisition card has a fixed number of digits for digitization and the wider the measurement range, the lower the resolution. Therefore it is also beneficial to adjust the data acquisition card measurement range with the signal amplitude range to obtain the best signal resolution available, this is achieved by adjusting the gain settings of the DAQ card.

An iterative auto-calibration scheme is made available in the ABS system to achieve the above functionalities. It iteratively checks for saturation and received signal amplitude, and then adjusts the analog output signal amplitude and the gain setting of the DAQ card to achieve the strongest emitted signal without saturation and the best signal resolution for the received signal.

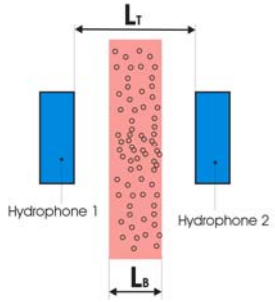

Fig. 8 Bubbly layer between two hydrophones

4 IMPROVEMENT OF DATA ANALYSIS

4.1 Spatial correction

It is not unusual that bubbles are not uniformly distributed between the two hydrophones in ABS experiments, instead they only distributed in a layer that only covers partially the space between the two hydrophones. The assumption of uniformity of bubble distribution between the two hydrophones in the data

analysis process will underestimate the actual bubble size distributions. The following analysis addresses this issue. Consider a bubbly layer between two hydrophones as shown in Fig. 8, and the measured quantities of u and v are u_m and v_m respectively. From Eq. 4~5 we have:

$$(u_m - iv_m)^2 = 1 + 4\pi C_l^2 \int \frac{aN_{uniform}(a)}{\omega_o^2 - \omega^2 + 2ib\omega} da, \quad (9)$$

where $N_{uniform}(a)$ corresponds to uniformly distributed bubbles between the two hydrophones. $N_{uniform}(a)$ is related to the real bubble density , $N(a)$, by:

$$N_{uniform}(a) \equiv \frac{L_B}{L_T} N(a) = \xi N(a), \quad (10)$$

where ξ is a spatial correction factor.

From Eq. 9~10 we get

$$(u_m - iv_m)^2 = 1 + \xi 4\pi C_l^2 \int \frac{aN(a)}{\omega_o^2 - \omega^2 + 2ib\omega} da, \quad (11)$$

If we notice that

$$(u_k - iv_k)^2 = 1 + 4\pi C_l^2 \int \frac{aN(a)}{\omega_o^2 - \omega^2 + 2ib\omega} da, \quad (12)$$

where the u_k and v_k are the quantities for uniform bubble distribution, $N(a)$, we obtain:

$$(u_m - iv_m)^2 = 1 + \xi\left[(u_k - iv_k)^2 - 1\right]. \quad (13)$$

This gives the corrected u_k and v_k as:

$$u_k = \sqrt{\left(A + \sqrt{A^2 + 4u_m^2 v_m^2}\right) \Big/ \sqrt{2\xi}}, \quad (14)$$

$$v_k = \frac{v_m}{\sqrt{\xi}} \sqrt{\frac{1-\xi}{v_m^2 + \xi u^2} + 1}, \quad (15)$$

where $A = u_m^2 - v_m^2 - 1 + \xi$.

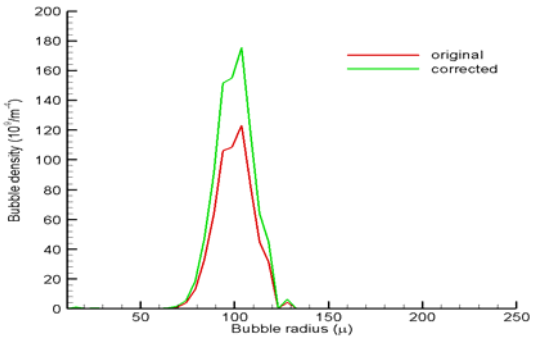

Fig. 9 Spatial correction effect on bubble density distribution

This spatial correction scheme was added in the ABS to handle bubble thick sheets between hydrophones. Fig. 9 shows an example of the effects of spatial correction ξ =0.8 on a bubble density distribution. The corresponding void fraction was also changed from 1.3 x 10^{-5} to 1.85 x 10^{-5}.

4.2 Iterative method to improve *u* measurements

In ABS measurements the quantities of u and v are calculated as follows for wave frequency $f = \omega/2\pi$:

$$u(f) = \Delta t_T / \Delta t_{ref}, \quad (16)$$

$$v(f) = \frac{c_{ref} log[\overline{p_T^2}(f) / \overline{p_{ref}^2}(f)}{4\pi f d_{ER}}. \quad (17)$$

Δt is the time for the acoustic wave to travel between hydrophones separated by a distance d_{ER}, $\overline{p^2}$ is the mean square amplitude of the pressure signal, and subscripts *ref* and *T* indicate measurements taken under either *reference* or *test* conditions. A correlation technique is used to compute Δt from the emitted and received signals, determination of Δt from the correlation peaks becomes more difficult as the signal to noise ratio deteriorates in the bubbly medium. In comparison, measurement of attenuation, v, is more accurate. To take advantage of the good v measurements, an iterative method is developed to improve the u measurements. At the first iteration step, *i=1*, assume u_1 = 1. and feed it with the measured v to the inverse problem solver to obtain a bubble density distribution, $N_i(a)$, as an approximation of the actual bubble size distributions. The sound speed ratio for the next time step, u_{i+1}, can be obtained from the following equation

$$u_{i+1} = B / v, \quad (18)$$

where *B* is the integral on the right hand side of Eq. 5. The above steps are performed iteratively until the of sound speed ratio values converge.

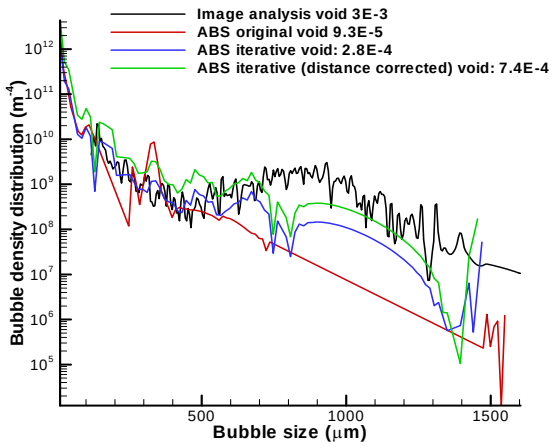

Fig. 10 An iterative scheme combined with spatial correction improves the measurement of bubble density distribution

The converged values u_{iti} are then used backwards to help choose the correlation peaks for Δt such that u obtained from Eq. 16 are closest to u_{iti}. Then u and v are used in the inverse problem solver to obtain the final solution of bubble density distribution.

This iterative algorithm improves the inverse solver stability and accuracy. Fig. 10 shows a comparison of such measurements with an optical method results. The ABS measurements obtained from the analysis that utilizes the iterative method and spatial correction compare best with the optical measurement.

4.3 Coupling with an interpolation scheme

The relationship between the number of bubble radii and the number of test frequencies affects the inverse solution. If the number of bubble radii selected in the inverse problem is greater than the number of frequencies used in the tests, the bubble distribution at several radii is zero and large spurious oscillations are present. Different interpolation schemes to expand the u and v values over a number of frequencies larger than the number of bubble radii were tested. Among these, the linear interpolation scheme was found to result in a similarly poor bubble distribution as that without using any interpolation , however a 3rd order cubic spline interpolation scheme, which allows for a continuous first and second derivative of the u and v curves, yields the best results.

This is illustrated in Fig 11. The exact curve represents the bubble density used to compute u and v for 40 frequencies. The bubble size range was discretized evenly over 150 radii. If the u and v curves are not interpolated, the bubble density is limited to 40 non-zero values. The interpolation procedure allowed for 150 additional frequencies. The linear interpolation resulted in an oscillating solution much like the non-interpolated case. The cubic interpolation clearly presented a superior solution that can support a fine resolution of the bubble density with minimal spurious oscillations.

5 EXPERIMENTAL VALIDATION

With recent developments in both hardware and software such as described above, the measurement range and accuracy of the ABS Acoustic Bubble Spectrometer®© system have improved significantly. To validate the accuracy of the system we have conducted many experiments and compared them with an optical method, mainly high-speed photography and image analysis, similar to those used in our previous studies [12-13].

Various methods, including electrolysis and air injection through porous material of various size, were used to generate uniform bubble distributions in the test volume between the hydrophones.

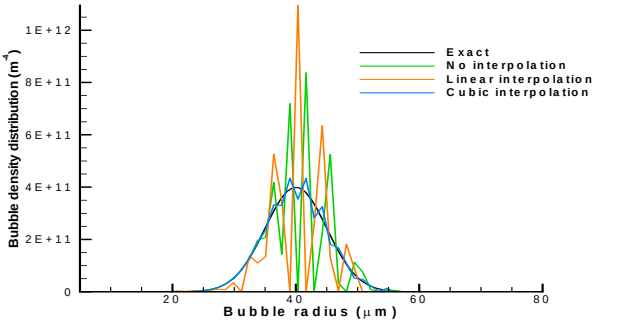

Fig. 11 Comparison of the effects of different interpolation schemes on the inverse solver

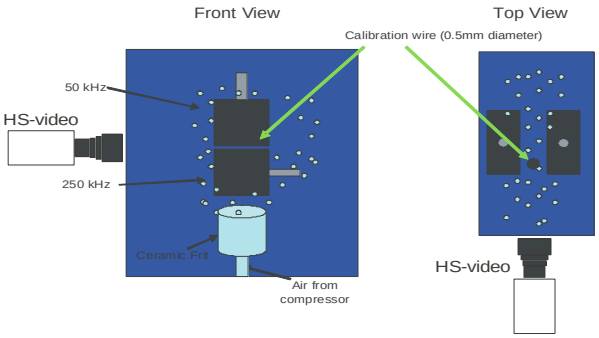

Fig. 12 Experiment setup for validating a twin-set ABS Acoustic Bubble Spectrometer® system

Fig. 12 shows a sketch of a setup for validating the ABS system. The optical measurements were obtained from two high speed video cameras focused on the same volume between two hydrophones. Different zoom lenses were used, such that both large and small bubbles could be captured. A calibration wire was used for scaling calibration. For validation, the ABS and the two HS-video cameras were synchronized so that the video cameras recorded while the ABS acquired signals. Validation experiments were conducted using an ABS system with two 250 kHz hydrophones. The hydrophones were 7 cm apart and the bubbles were generated using an electrolysis wire grid. Fig. 13 compares the results from the ABS with those from optical measurement. The two agree well with each other and give similar bubble size distribution and the total measured void fraction is about 1.2 x 10^{-4}.

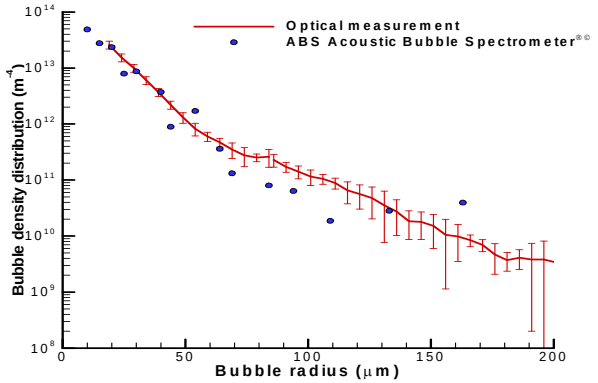

Fig.13 Comparison of bubble population density measurements from a single-set ABS system and a high-speed photography system

Experiments were performed to verify the effectiveness of using a multiple-set ABS system for measurements in higher void fraction conditions. Two sets of hydrophones, a 50 kHz pair and a 250 kHz pair, were used, the hydrophones were set 6 cm apart. Bubbles were generated by pumping air with a compressor through a porous sintered steel tube. The tube was placed such that the created bubbles completely filled the test volume between the two pairs of hydrophones.

Fig. 14 shows a comparison of the measurements results from the two methods. The distribution computed by the ABS also followed closely the one obtained from the photography. The void fraction obtained in this case is 2.5 x 10^{-3}.

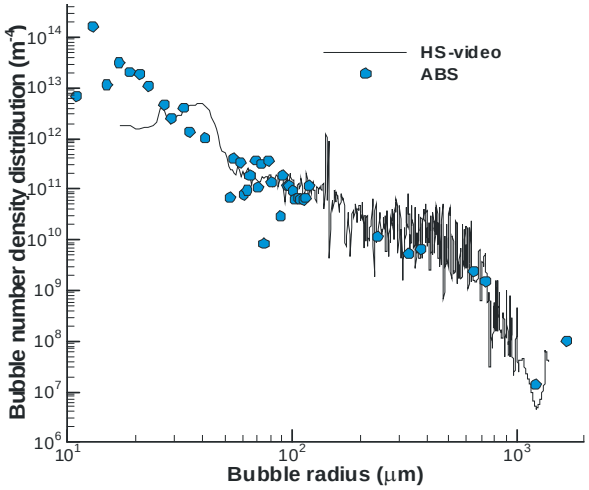

Fig. 14 Comparison of the bubble density distribution between a twin-set ABS and HS-video measurements at higher void fraction conditions.

6 CONCLUSIONS

The ABS Acoustic Bubble Spectrometer®© is an acoustics-based device, which provides bubble size distribution in a bubbly liquid through measurement of the sound speed and attenuation at various frequencies and solution of an inverse problem using the measured quantities. Recent developments of this instrumentation method from many perspectives, in both hardware and software, have significantly improved its measurement range and accuracy, as well as system robustness. Extensive validation experiments were conducted by comparing against an optical method using high speed video photography. The comparison indicates that the two methods give very close results for void fractions up to 3x10^{-3} with bubble sizes ranging from 10 μm to 3 mm.

ACKNOWLEDGEMENTS

We are grateful for partial support by the National Science Foundation and Oak Ridge National Laboratory to develop the ABS. We also thank the many people at DYNAFLOW who contributed to the extensive developments.

REFERENCES

[1] Medwin H. Counting bubbles acoustically: a review. Ultrasonics, 1977, 15: 7-13.
[2] MacIntyre F. On reconciling optical and acoustical bubble spectra in the mixed layer," in "Oceanic Whitecaps. edited by Monahan, E.C. and Macniocaill, G., Reidell, New York, 1986:75-94.
[3] Wildt R editor. Physics of Sound in the Sea, Part IV. National Research Council, 1949.
[4] Breitz N, Medwin H. Instrumentation for in situ acoustical measurements of bubble spectra under breaking waves. J. Acoust. Soc. Am., 1989, 86: 739-743.
[5] Oldenziel D M. A new instrument in cavitation research: the cavitation susceptibility meter. J. Fluids Engg., 1982, 104:136-142.
[6] Vagle S, Farmer D M. The measurement of Bubble-Size Distributions by Acoustical Backscatter. J. Atmos. Ocean. Tech., 1992, 9: 630-644.
[7] Ohern T, Torczynski J, Tassin S, et al. Development of an Electrical Impedance Tomography System for an Air-Water Vertical Bubble Column. Proceedings, Forum on Measurement Techniques in Multiphase Flows, ASME IMECE, San Francisco, CA, USA, 1995.
[8] Hsiao C -T, Chahine G, Gumerov N. An efficient electrical impedance tomography software combining boundary element method and genetic algorithm. OptiCON'99, Optimization Software, Methods, and Applications Conference Proceedings, Newport Beach, California, USA, 1999.
[9] Gumerov N A, Chahine G L, Goumilevski A G. Dipole approximation method and its coupling with the regular boundary element method for efficient electrical impedance tomography. in "Boundary Element Technology XIII," edited by Chen, C.S., Brebbia, C.A. and Pepper, D.W., WIT Press, Southampton, UK, 1999: 217-226.
[10] Prabhukumar S, Duraiswami R, Chahine G L. Acoustic measurement of bubble size distributions: theory and experiments. ASME Cav. Multi. Flow F., 1996: 509-514.
[11] Duraiswami R, Prabhukumar S, Chahine G L. Bubble counting using an inverse acoustic scattering method. J. Acoust. Soc. Am., 1998, 104: 2699-2717.
[12] Chahine G, Kalumuck K, Cheng J –Y, et al. Validation of Bubble Distribution Measurements of the ABS Acoustic Bubble Spectrometer® with High Speed Video Photography. 4th Intern. Symp. Cav., CAV2001, 2001, Pasadena, CA, USA.
[13] Chahine G, Kalumuck K. Development of a Near Real-Time Instrument for Nuclei Measurement: the ABS Acoustic Bubble Spectrometer®. Joint ASME/JSME Fluids Engineering Conference, Honolulu, Hawaii, USA, 2003.
[14] Caflisch R E, Miksis M J, Papanicolau G C, et al. 'Effective Equations for wave propagation in bubbly liquids. J. Fluid Mech. 1985, 153: 259-273.
[15] Commander K W, Prosperetti A. Linear pressure waves in bubbly liquids: Comparison between theory and experiments. J. Acoust. Soc. Am., 1989, 85: 732-746.